Advances in Aerospace Science and Applications.
ISSN 2277-3223 Volume 11, Number 1 (2021), pp. 1-10

http://www.ripublication.com

Velocity Perturbations Analysis of the Fragmentation of USA-193 Satellite in Orbit

Arjun Tan[1] **and Robert C. Reynolds**[2]

[1]*Department of Physics, Alabama A & M University, Normal, AL 35762, U. S. A.*

[2]*VP for Advanced Programs, STAR Dynamics Inc., Hilliard, OH 43026, U.S.A.*

Abstract

The radar imaging U.S. military reconnaissance satellite USA-193, launched on 14 December 2006 into a low-Earth orbit, malfunctioned shortly afterwards with its hydrazine propellants unused. In order to mitigate the possible adverse effects of the toxic fuel upon the satellite's atmospheric re-entry, it was destroyed by kinetic impact launched from an SM-3 missile above the Pacific Ocean on 21 February 2008 similar to one conducted in an anti-satellite event. This paper interprets the satellite fragmentation event by calculating and analyzing the velocity perturbations of 170 fragments cataloged through 21.38 days following the breakup. The fragments dispersion was easily the most lopsided and anisotropic amongst all breakup events studied by the authors. The most striking features of the fragment counts are the following: 90% of all fragments were ejected above the horizontal plane; 80% of all fragments were ejected in the forward direction; and an equal number of fragments were ejected to the left and right of the parent satellite when viewed from above. Octant I contained the highest proportion (41%) of the fragments, followed by Octant IV (39%). Thus 80% of all fragments were confined in the two adjacent octants above the horizontal plane. Right below them, no fragments were found in either of Octants V and VIII. Three fragments 32686, 32687 and 32899 with the highest velocity changes were thrown in the negative cross-range direction of the fragmenting satellite. They were recognized as being analogous to the 'anomalous objects' observed in the Solwind P78-1 fragmentation. They also displayed the phenomenon of 'sequential fragmentation' in space. The 'center-of-mass' of the debris cloud was ejected at an amazing speed of 186.67 m/s from the parent, a result never encountered in a satellite breakup before. The small kinetic kill vehicle of the SM-3 missile could not have produced such a debris cloud out of the massive USA-193 satellite by impact alone. The only possible way for this to happen would be for the hydrazine tank to be situated

at one end of the satellite and suffer a massive explosion in the 'clam' model of the explosive fragmentation of orbiting propellant tanks.

INTRODUCTION

On 14 December 2006, the radar imaging U.S. military reconnaissance satellite ***USA-193*** (International Designator 2006-057A; U.S. Satellite Number 29651) was launched for the National Reconnaissance Office into a low-Earth orbit [1]. The satellite was thought to be 4.6 m long and 2.4 m wide and reportedly weighed about 2,300 kg [2]. It malfunctioned shortly after deployment and as its orbit decayed sufficiently with its hydrazine propellants unused, it was feared that the satellite could survive re-entry into the atmosphere and spew toxic hydrazine into the environment [3]. In order to mitigate this possibility, it was decided to destroy the satellite by kinetic impact in space before its re-entry into the atmosphere [3]. This happened on 21 February 2008 when a modified SM-3 missile from the U.S. Navy warship Lake Erie struck the satellite over Pacific Ocean at an altitude of 247.769 km, latitude 8.813°N and longitude 189.023°E, thereby thoroughly fragmenting it [1]. The event was reminiscent of the destruction of Solwind P78-1 satellite in 1986 and the Fengyun-1C satellite in 2007 in the anti-satellite tests conducted by the United States of America and People's Republic of China, respectively. Even though the USA-193 fragmentation was not designated as an anti-satellite test, it may not be distinguishable from one. In this paper, we examine the USA-193 fragmentation by (1) examining the ***Gabbard diagram*** of the fragments produced; and (2) calculating and analyzing the ***magnitudes and directions of the fragment velocities***. The method of Badhwar, et al. [4] is used for the latter purpose. The orbital elements of USA-193 remain classified, but the relevant information about its last orbit prior to the breakup were calculated from the event location data found in the literature [1]. The data for the orbital elements of the fragments are available from *Space-track.org* [5].

METHOD OF ANALYSIS

The magnitude, variance and directionality of the ejection velocities of the fragments can shed valuable light regarding the nature and intensity of the fragmentation. Badhwar, et al. [4] obtained exact solutions for the velocity perturbations of the fragments of a breakup. In an orthogonal coordinate system with the fragmenting satellite at the origin and the radial (r), down-range (d) and cross-range (x) directions as the axes, the velocity of the parent satellite at the instance of fragmentation is written as $\vec{v} = v_r \hat{r} + v_d \hat{d}$, where

$$v = \sqrt{\mu\left(\frac{2}{r} - \frac{1}{a}\right)} \tag{1}$$

$$v_d = \frac{1}{r}\sqrt{\mu a\left(1 - e^2\right)} \tag{2}$$

and

$$v_r = \pm\frac{1}{r}\sqrt{\mu a e^2 - \frac{\mu}{a}(r-a)^2} \tag{3}$$

In Eqs. (1) – (3), a is the semi major-axis and e the eccentricity of orbit; r is the radial distance from the center of the Earth; and μ is the gravitational parameter of the Earth. In Eq. (3), the + sign corresponds to the ascending mode of the satellite (true anomaly $\theta < \pi$) whereas the – sign corresponds to the descending mode ($\theta > \pi$).

Upon fragmentation, the velocity of a fragment has the components $v_r + dv_r$, $v_d + dv_d$ and dv_x, with dv_r, dv_d and dv_x being the velocity perturbation components of the fragment [4]:

$$dv_r = \pm\sqrt{\mu\left(\frac{2}{r} - \frac{1}{a'}\right) - \frac{\mu}{r^2}a'\left(1-e'^2\right)} - v_r \tag{4}$$

$$dv_d = \frac{\cos\xi}{r}\sqrt{\mu a'\left(1-e'^2\right)} - v_d \tag{5}$$

and

$$dv_x = \frac{\sin\xi}{r}\sqrt{\mu a'\left(1-e'^2\right)} \tag{6}$$

In Eq. (4), the + sign corresponds to the ascending mode of the fragment (true anomaly $\theta' < \pi$), whereas the – sign corresponds to the descending mode ($\theta' > \pi$).

In Eqs. (5) and (6), ξ is the plane-change angle of the fragment given by [4]:

$$\xi = \pm\cos^{-1}\frac{\cos i\cos i' + \sqrt{\cos^2\lambda - \cos^2 i}\sqrt{\cos^2\lambda - \cos^2 i'}}{\cos^2\lambda} \tag{7}$$

where λ is the latitude of the fragmentation point. In Eq. (7), the + sign corresponds to $i' > i$ and the – sign corresponds to $i' < i$ on the northbound orbits with the opposite sense on the southbound orbits, i and i' being the inclinations of the parent and fragment, respectively.

The true anomaly θ' of the fragment, which dictates the sign of dv_r, is determined from the argument of latitude u' and the argument of perigee ω' of the fragment at the time of the breakup as: $\theta' = u' - \omega'$. Since the argument of perigee is perturbed by the oblateness of the Earth, the argument of perigee at the time of observation ω_0' is different from its value at the time of fragmentation ω'. From the rate of precession, one has [6]:

$$\omega' = \omega_0{}' - 4.98\left(\frac{R}{a}\right)^{7/2}\frac{5\cos^2 i - 1}{(1-e'^2)^2}dt \tag{8}$$

where R is the reference radius of the Earth (6,378.137 km), dt is the time of observation from the time of fragmentation in days, and ω' and ω_0' are expressed in degrees.

The velocity perturbation components dv_d, dv_x and dv_r may be used to define various planes and quarters of space. For example, dv_d and dv_x define the local horizontal plane; and dv_r, and dv_d define a vertical plane which is the plane of the orbit. dv_r, and dv_x define the other vertical plane perpendicular to the plane of the orbit. Two angular coordinates are defined as follows: (1) the ***latitude*** λ, measured from the horizontal plane; and (2) the ***longitude*** ϕ, measured from the plane of the orbit:

$$\lambda = \sin^{-1}\left(\frac{dv_r}{dv}\right) \tag{9}$$

and

$$\phi = \tan^{-1}\left(\frac{dv_x}{dv_d}\right) + n\pi \tag{10}$$

where $n = 0$ if $dv_d > 0$; $n = 1$ if $dv_d < 0$ and $dv_x > 0$; and $n = -1$ if $dv_d < 0$ and $dv_x < 0$. λ ranges from $-\pi/2$ to $\pi/2$; whereas ϕ ranges from $-\pi$ to π. The eight ***octants of space*** are defined in accordance to the scheme indicated in Table I.

Table I. Fragment counts in various quarters of space

Fragments in regions of space	dv_d	dv_x	dv_r	Count	%
Fragments in all space	all	all	all	170	100
Fragments ejected upwards	all	all	+	153	90
Fragments ejected downwards	all	all	–	17	10
Fragments ejected forwards	+	all	all	136	80
Fragments ejected backwards	–	all	all	34	20
Fragments ejected to the left*	all	+	all	85	50
Fragments ejected to the right*	all	–	all	85	50
Fragments ejected in Octant I	+	+	+	69	41
Fragments ejected in Octant II	–	+	+	10	6
Fragments ejected in Octant III	–	–	+	7	4
Fragments ejected in Octant IV	+	–	+	67	39
Fragments ejected in Octant V	+	+	–	0	0
Fragments ejected in Octant VI	–	+	–	6	4
Fragments ejected in Octant VII	–	–	–	11	6
Fragments ejected in Octant VIII	+	–	–	0	0
*looking downwards from the parent satellite at fragmentation					

RESULTS

The orbital elements of USA-193 remain classified as of now. However, its last orbit prior to impact can be constructed from bits of data found in the open literature. For example, we have: the apogee height h_a = 257 km; perigee height h_p = 241 km; inclination i = 58.48° [7]; and event date and time, 21 February 2008 0326 GMT [1]. From the basic equations of the orbital ellipse, one gets: a = 6,627.645 km; e = .001131624; and true anomaly θ = 76.7189° (ascending mode); whence by Eqs. (1) – (3): v = 7.757166447 km/s; v_d = 7.757161747 km/s; and v_r = 8.53952 m/s.

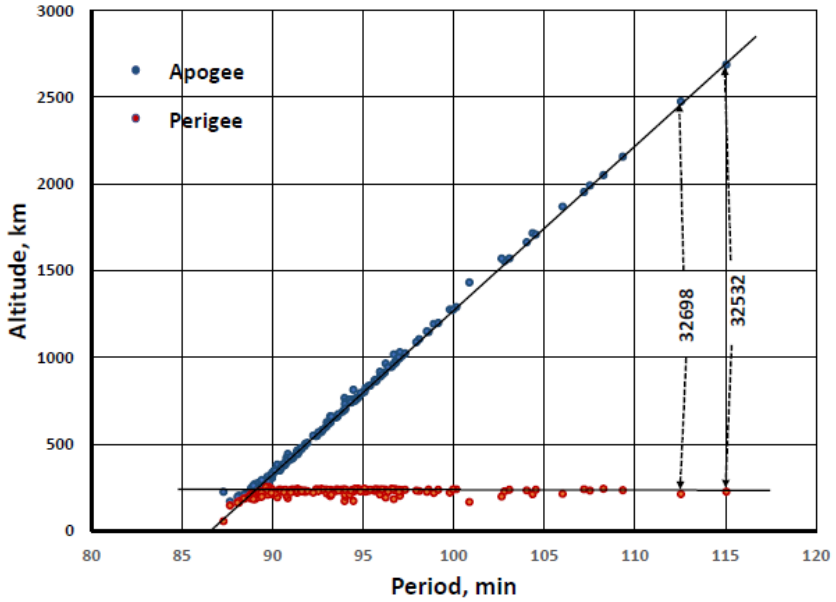

Fig. 1

Figure 1 is the Gabbard diagram of 170 fragments of USA-193 cataloged through 21.38 days following the breakup. During that period, 203 fragments (serial numbers 32502 consecutively through 32704) were urgently tracked, out of which 170 were cataloged, the rest presumably having de-orbited early. The Gabbard diagram plots the apogee and perigee heights (h_a and h_p, respectively) of each fragment against its orbital period P. For a breakup occurring in a nearly circular orbit at a relatively low altitude, the typical Gabbard diagram shows an inclined 'X' form, with its left arms largely missing and acquiring a 'claw shape'. In this case, the left arms are almost completely missing, whereby suggesting that most of the fragments with negative dv_d's had deorbited rapidly. The two fragments on the far right (32698 and 32532) on the other end received the highest dv_d's in the positive down-range direction.

The fragments dispersion in the USA-193 breakup event was easily the most lopsided and anisotropic amongst all breakup events studied by the authors. The fragment counts in the various quarters of space are compiled in Table I. The most striking features of the fragment counts are the following: (1) 90% of all fragments were ejected above the horizontal plane and the remainder 10% below it; (2) 80% of all fragments were ejected

in the forward direction and only 20% in the retrograde direction; and (3) An equal number of fragments were ejected to the left and right of the parent satellite when viewed from above. Octant I contained the highest proportion (41%) of the fragments, followed by Octant IV (39%). Thus 80% of all fragments were confined in the two adjacent octants above the horizontal plane. Right below them, no fragments were found in either of Octants V and VIII.

Table II. Velocity perturbations of the Fragments

	dv_d, m/s	dv_x, m/s	dv_r, m/s	dv, m/s
Maximum	572.68	279.73	340.04	942.56
Minimum	−121.73	−941.25	−8.54	18.81
Average	106.62	−22.49	76.35	186.67
Range	694.41	1,220.98	348.58	923.75

Table II shows the highest, lowest and average values of the dv_d, dv_x, dv_r and dv and their ranges. The large positive average values of dv_d and dv_r confirm the fact that most of the fragments were ejected in the forward and upward directions. The unusually wide range of the dv_x values were due to three fragments (32686, 32687 and 32899), reminiscent of the three '***anomalous objects'*** observed in the Solwind P78-1 fragmentation [8], which were later recognized as '***ricochet fragments***' produced by hypervelocity impact [9]. These three fragments had the highest ejection speeds amongst all fragments (Table III, which also includes the next seven fragments). However, unlike the Solwind anomalous objects, they do not stand out in the Gabbard diagram like the fragments 32532 and 32698 (Fig. 1), which had the next highest dv values (Table III). The reason for this is that their dv_d values were negative, which did not act in enhancing their orbital periods.

Table III. Fragments with largest Velocity Changes

Fragment #	dv_d, m/s	dv_x, m/s	dv_r, m/s	dv, m/s
32686	−49.01	−941.25	−8.54	942.56
32687	−53.00	−940.94	−8.54	942.47
32699	−121.73	−933.81	−8.54	941.75
32532	572.68	4.54	236.13	619.47
32698	525.21	−59.11	296.68	606.10
32583	467.84	92.70	162.92	504.00
32591	430.68	158.15	172.03	400.00
32502	282.10	−176.42	340.04	475.75
32503	399.11	−27.27	252.85	473.25
32597	448.50	28.80	94.56	459.26

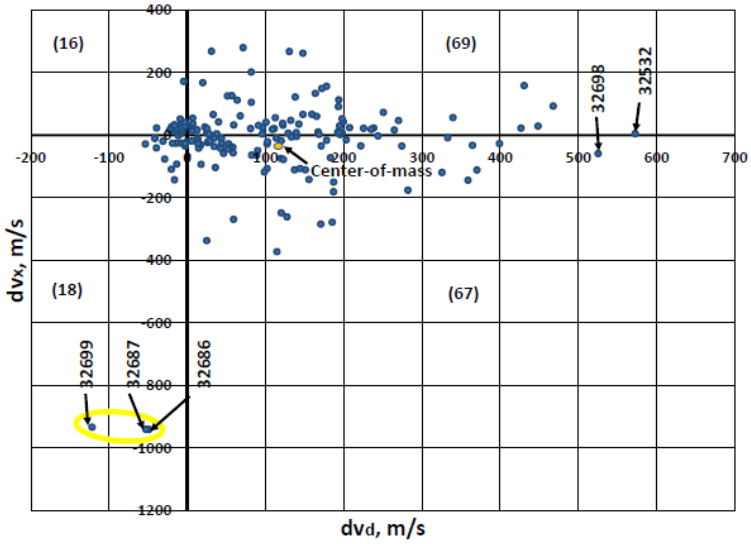

Fig. 2

Figure 2 is a scatterplot of the fragments in the horizontal dv_x– dv_d plane as viewed from above. Fragments having the largest dv_d's (32698 and 32532) are marked on the far right. The fragments 32699, 32687 and 32686 having the highest dv's are shown on the lower left corner. They were ejected to the far right of the fragmenting satellite path seen from above. Also shown in the figure is the 'center-of-mas' having the average dv values, i.e., with each fragment weighted equally. Since all fragments were reportedly small ('not larger than an American football') [2], this characterization is not an unfair one. The numbers of fragments in each quadrant of space are marked in Fig. 2. Clearly, the first and fourth quadrants contained the vast majority of the fragments.

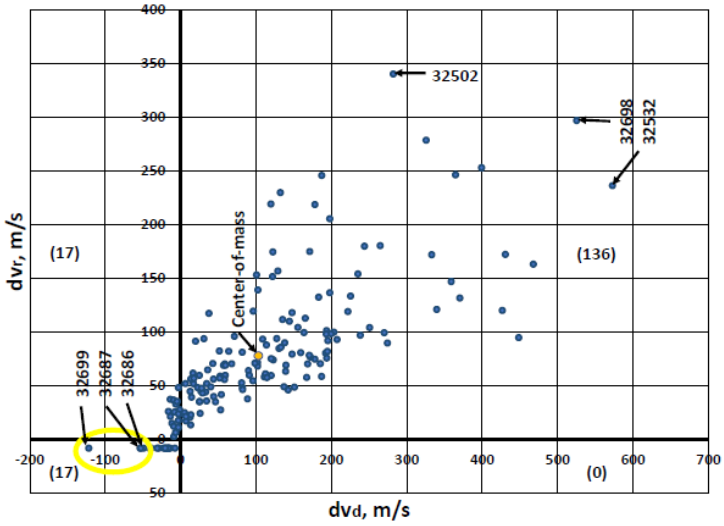

Fig. 3

Figure 3 is a scatterplot of the fragments in a vertical plane containing the orbit of the fragmenting satellite, which is the dv_r– dv_d plane. The fragments 32698 and 32532 take

their prominent places in the first quadrant which contains an astonishing 136 out of 170 (or 80%) of all fragments. The anomalous fragments (32699, 32687 and 32686) take a lowly backseat in the third quadrant, on the verge of imminent re-entry into the atmosphere. The slope of the center-of-mass of the fragments in this $dv_r - dv_d$ orbital plane is a steep (vide Table II) $\tan^{-1}(76.35/106.62) = 35.6^o$. The actual slope of the center-of-mass cloud from the horizontal plane is, however (from Eq. 9) $\sin^{-1}(76.35/186.67) = 24.14^o$. The latter angle is suggestive of the slope of the interceptor when it hit its target.

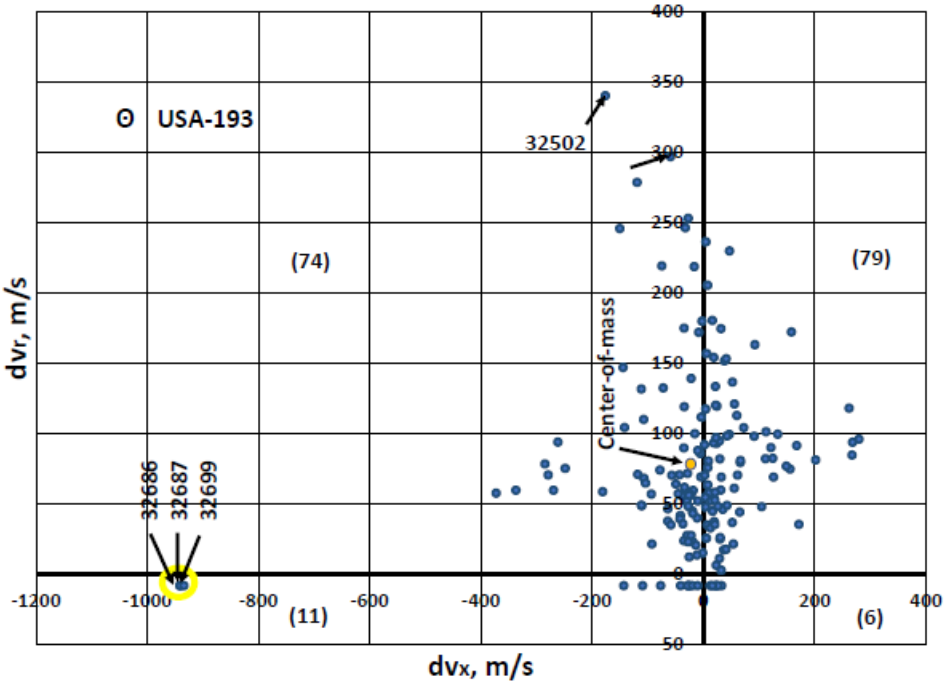

Fig. 4

Figure 4 is the scatterplot of the fragments in a second vertical plane containing the orbital angular momentum vector of the fragmenting satellite, which is the $dv_r - dv_x$ plane. Its features are consistent with those of Figs. 2 and 3. The direction of the parent satellite is vertically out of the plane. A full 90% of the fragments were found in the first two quadrants, with a slightly higher number in the first quadrant (79) than in the second (74). However, the center-of-mass of the fragments was slightly inside the latter quadrant, due perhaps to the three anomalous fragments far flung to the left. These fragments are now bunched tightly together, unlike in Figs. 2 and 3, where there was a substantial gap between 32699 on one hand and 32686 and 32687 on the other. This may well be a classic example of ***sequential fragmentation in space***, first proposed by Brown [10] and later observed by Tan, et al. [9] in the Solwind P78-1 fragmentation by kinetic impact. The likely scenario played out is as follows: A large chunk of fragment breaks out off the target, which first fragments into two pieces, one fragment 32699 and the other still a composite of 32686 and 32687; and the latter subsequently undergoing a second fragmentation into 32686 and 32687.

The angular distributions of the USA-193 fragments are shown on Lambert's equidistant cylindrical projection map in Fig. 5. The numbers of fragments in each of the eight octants are marked. Most fragments were found in Octant I (69 or 41%) followed by in Octant IV (67 or 39%) with the two octants accounting for 80% of the fragments. Right below them, there were no fragments in octants V and VIII. Overall, there were 153 fragments (90%) above the horizontal plane and only 17 (10%) below the horizontal plane. The three anomalous fragments with the highest velocity changes (32686, 32687 and 32699) are bunched together near the four corners of Octants III, IV, VII and VIII. The fragment with highest dv_r (32502) is marked on the map as well as the fragment with the second highest dv_d (32698). Not far from the latter is located the center-of-mass of all fragments.

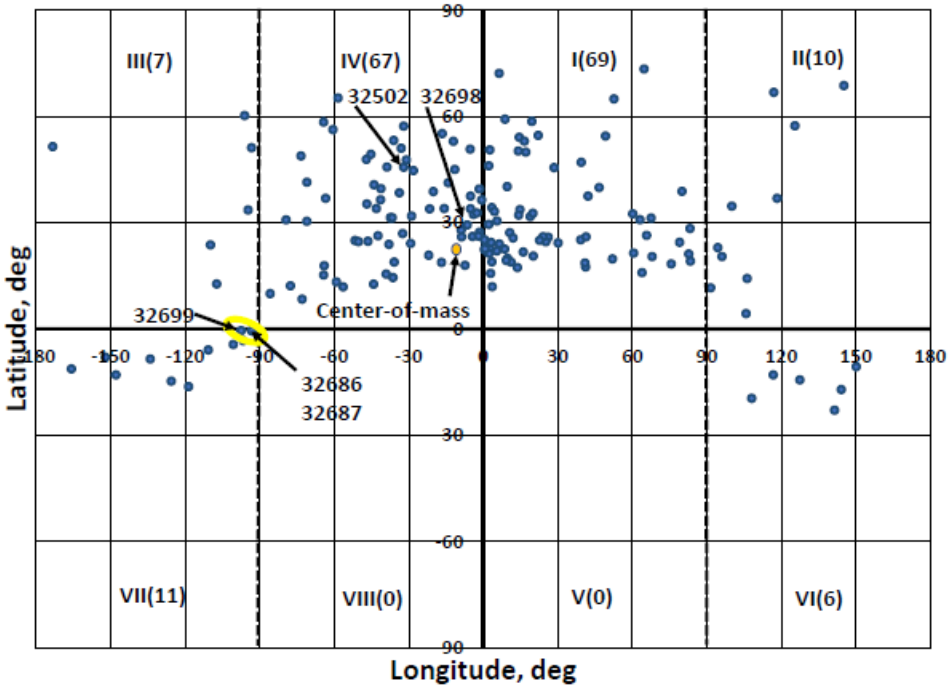

Fig. 5

DISCUSSION

The fragmentation of USA-193 by kinetic impact is like no other satellite fragmentation on record. With 90% of the fragments moving above the horizontal plane, 80% of the fragments moving the forward direction, and the center-of-mass of the cloud moving at an amazing speed of 186.67 m/s, this fragmentation is in a class by itself. The small kinetic kill vehicle of the SM-3 missile (LEAP) could not have produced such a debris cloud out of the massive USA-193 satellite by impact alone [11]. The only possible way for this to happen will be for the hydrazine tank to be situated at one end of the satellite and suffer a massive explosion in the '***clam model***' of the explosive fragmentation of orbiting propellant tanks [12].

REFERENCES

[1] P. Anz-Meador, J.N. Opiela, D. Shoots & J.-C. Liou, *History of on-orbit Satellite Fragmentation*, NASA/TM-2018-22037 (2018), p. 458.

[2] https://celestrak.com/events/usa-193.php.

[3] *Orbital Debris Quarterly News*, *12*(*2*), 1-2 (2008).

[4] G.D. Badhwar, A. Tan, & R.C. Reynolds, Velocity Perturbations Distributions in the Breakup of Artificial Satellites, *J. Spacecr. Rockets, 27*, 299-305 (1990).

[5] https://www.space-track.org/perl/id_query.pl

[6] D. King-Hele, *Satellite Orbits in an Atmosphere*, Blackie (Glasgow, 1987), p.6.

[7] https://en.wikipedia.org/wiki/USA-193.

[8] R. Kling, Postmortem of a hypervelocity impact, *Teledyne Brown Engineering Rept. CS86-LKD-001* (1986).

[9] A. Tan, G.D. Badhwar, F.A. Allahdadi & D.F. Medina, Analysis of the Solwind fragmentation using theory and computations, *J. Spacecr. Rockets*, *33*, 79-85 (1996).

[10] W.K. Brown, A theory of sequential fragmentation and its astrophysical applications, *J. Astrophys. Astronom.*, *10*, 89-112 (1989).

[11] http://web.mit.edu/stgs/pdfs/Forden_Preliminary_analysis_USA_193_ Shoot_down.pdf.

[12] F.J. Benz, R.L. Kays, C.V. Bishop & M.B. Eck, Explosive fragmentation of orbiting propellant tanks in *Orbital Debris from Upper Stage Breakup*, J.P. Loftus ed., AIAA, Washington (1989), pp. 107-129.